Supporting Information

Block sequence-specific glycopolypeptides with selective lectin binding properties

Cristina Lavilla*,[a] Gokhan Yilmaz,[b] Veselina Uzunova,[c] Richard Napier,[c] C. Remzi Becer,[b] Andreas Heise*,[a,d]

[a] Department of Chemical Engineering and Chemistry, Eindhoven University of Technology, Den Dolech 2, 5612AZ Eindhoven, The Netherlands

[b] Polymer Chemistry Laboratory, School of Engineering and Materials Science, Queen Mary University of London, London, E1 4NS, United Kingdom

[c] Life Sciences, University of Warwick, CV4 7AL, Coventry, United Kingdom

[d] Department of Pharmaceutical and Medicinal Chemistry, Royal College of Surgeons in Ireland, 123 St. Stephens Green, Dublin 2, Ireland

Table S1. Observed and calculated IR frequencies of the Amide I and Amide II bands of polypeptides in various conformations. Adapted from literature.[i]

		Wavenumber (cm^{-1})			
Conformation	Designation	Amide I (observed)	Amide I (calculated)	Amide II (observed)	Amide II (calculated)
Random coil		1656 (s)	1658	1535 (s)	1535
α-Helix	$v_{\parallel}$ (0) $v_{\perp}$ (2π/n)	1650 (s) 1652 (m)	1650 1647	1516 (w) 1546 (s)	1516 1540
β-Parallel-chain pleated sheet	$v_{\parallel}$ (0,0) $v_{\perp}$ (π,0)	1645 (w) 1630 (s)	1648 1632	1530 (s) 1550 (w)	1530 1550
β-Antiparallel-chain pleated sheet	$v_{\parallel}$ (0,π) $v_{\perp}$ (π,0) $v_{\perp}$ (π,π)	1685 (w) 1632 (s)	1685 1632 1668	1530 (s)	1530 1540 1550

n is the number of peptide groups per turn of the helix.
The observed intensities are indicated as follows: s, strong; m, medium; w, weak.

Table S2. Absorbance at 450 nm of samples prepared by adding 50 µL glycopolypeptide (1 mg/mL) into 500 µL solution (buffer, RCA_{120} or ConA). Concentration of RCA_{120} and ConA initial lectin solutions were 2 mg/mL.Data corresponds to absorbance recorded 60 minutes after addition.

Glycopolypeptide	Buffer	RCA_{120}		ConA	
	Abs	$Abs_{measured}$	$Abs_{corrected}$ [a]	$Abs_{measured}$	$Abs_{corrected}$ [a]
$[(GA)_5\text{-}(GalG)_5]_4$	0.02	0.25	0.23	0.03	0
$[(GA)_{10}\text{-}(GalG)_{10}]_2$	0.02	0.20	0.18	0.02	0
$(GA)_{20}\text{-}b\text{-}(GalG)_{20}$	0.03	0.14	0.11	0.02	0
$(GA)_{20}\text{-}st\text{-}(GalG)_{20}$	0.02	0.22	0.20	0.02	0
[a]Absorbance corrected for the effect of the buffer = $Abs_{measured} - Abs_{buffer}$					

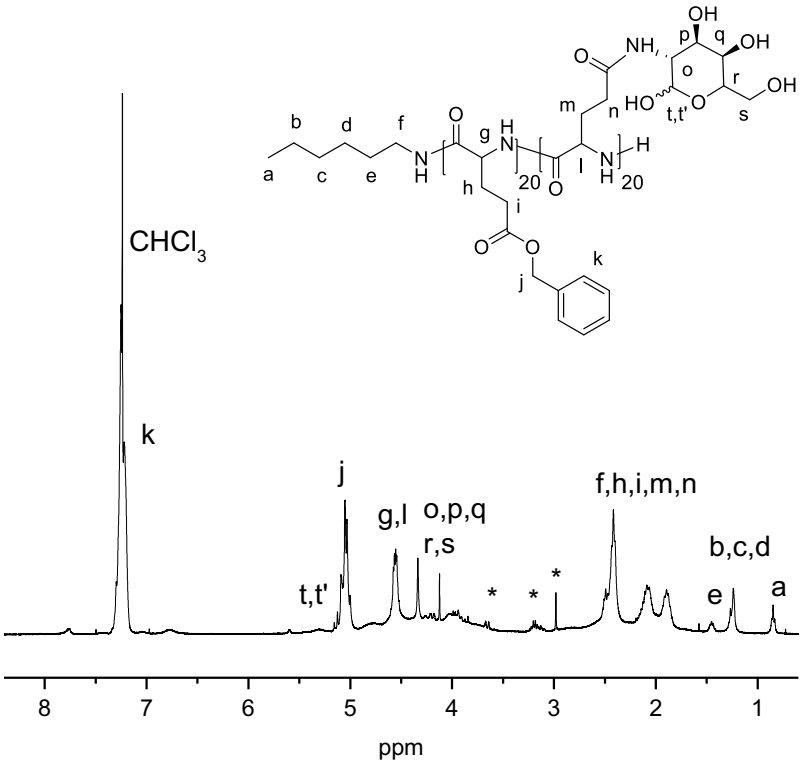

Figure S1. ^1H NMR of $(BG)_{20}\text{-}b\text{-}(GalG)_{20}$ in $CDCl_3$/TFA-*d*. The * corresponds to residues of DMT-MM.

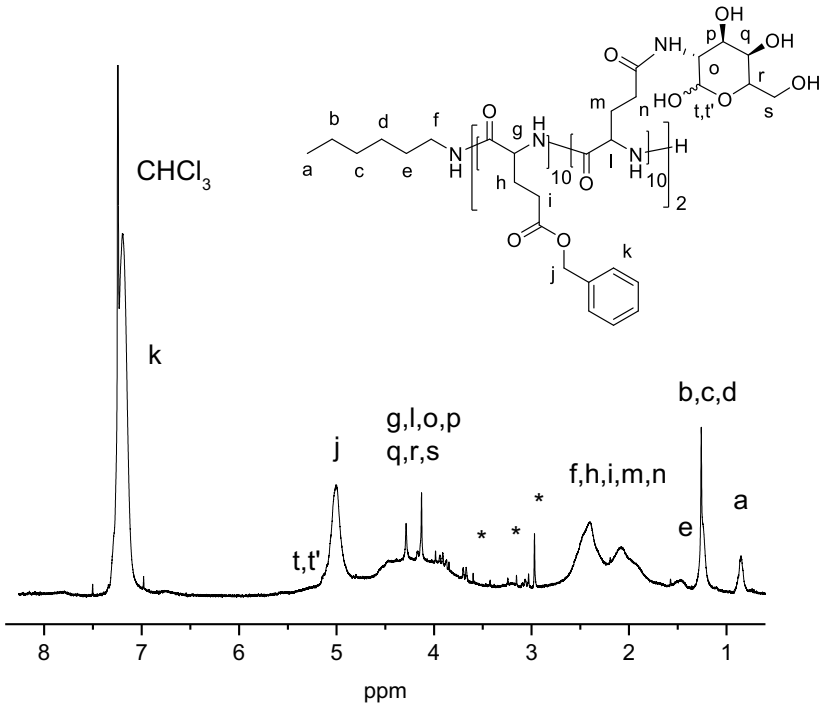

Figure S2. ^{1}H NMR of $[(BG)_{10}\text{-}(GalG)_{10}]_2$ in $CDCl_3$/TFA-*d*. The * corresponds to residues of DMT-MM.

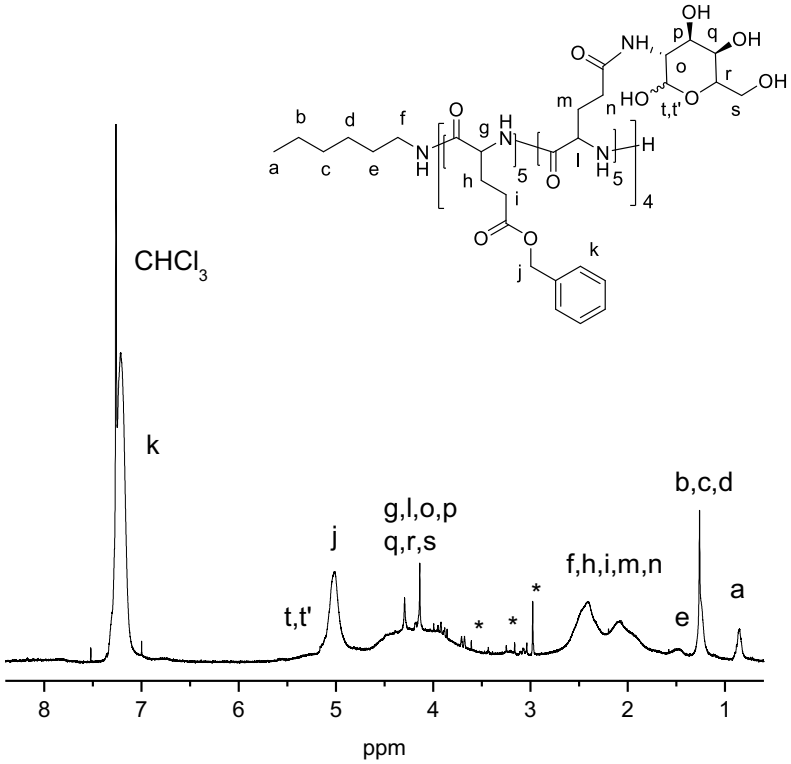

Figure S3. ^{1}H NMR of $[(BG)_5\text{-}(GalG)_5]_4$ in $CDCl_3$/TFA-*d*. The * corresponds to residues of DMT-MM.

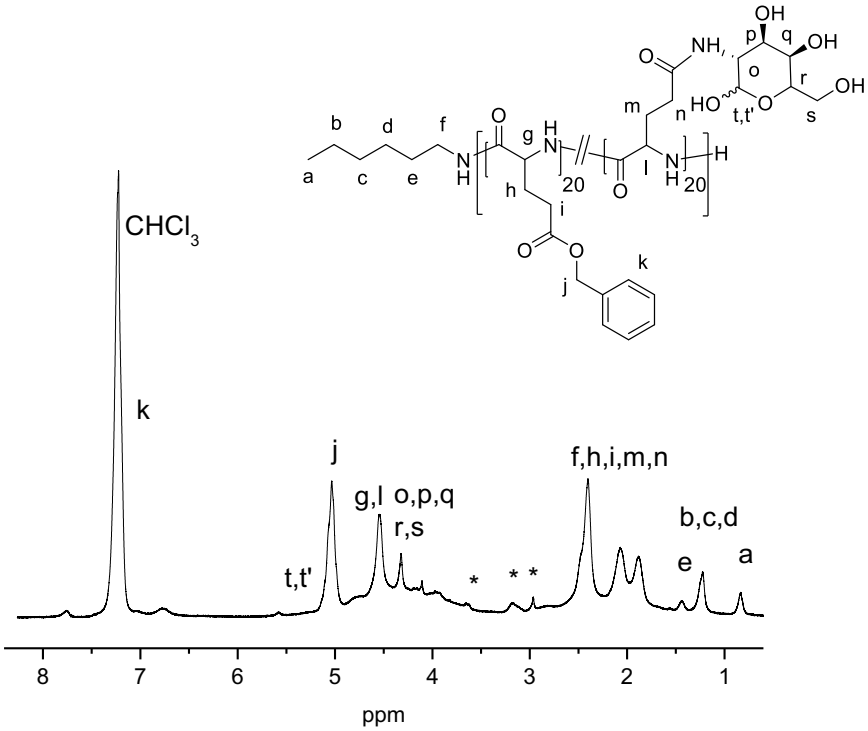

Figure S4. ^{1}H NMR of $(BG)_{20}$-*st*-$(GalG)_{20}$ in $CDCl_3$/TFA-*d*. The * corresponds to residues of DMT-MM.

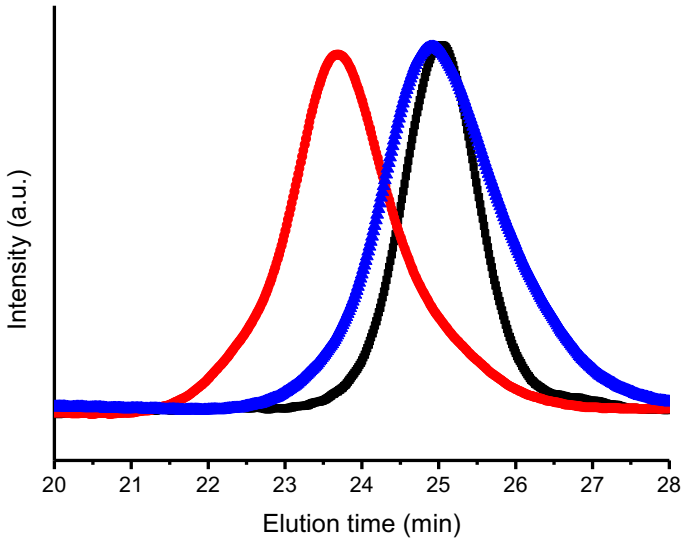

Figure S5. SEC traces of $(BG)_{20}$-*b*-$(TBG)_{20}$ (black), $(BG)_{20}$-*b*-$(GalG)_{20}$ (red) and $(GA)_{20}$-*b*-$(GalG)_{20}$ (blue).

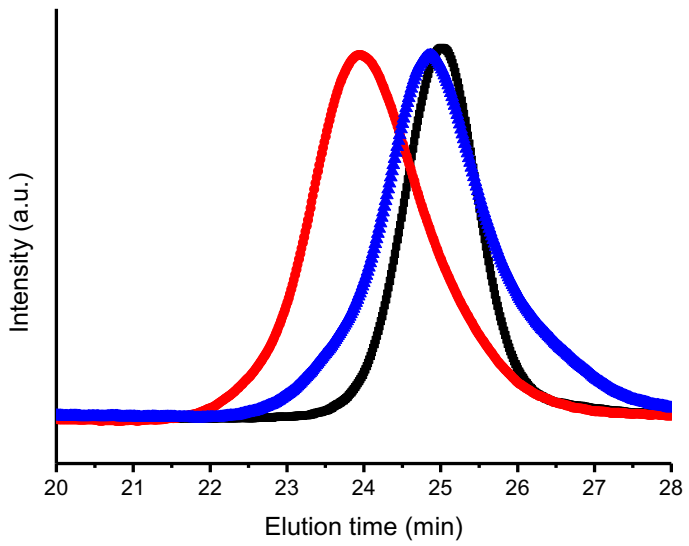

Figure S6. SEC traces of $[(BG)_{10}\text{-}(TBG)_{10}]_2$ (black), $[(BG)_{10}\text{-}(GalG)_{10}]_2$ (red) and $[(GA)_{10}\text{-}(GalG)_{10}]_2$ (blue).

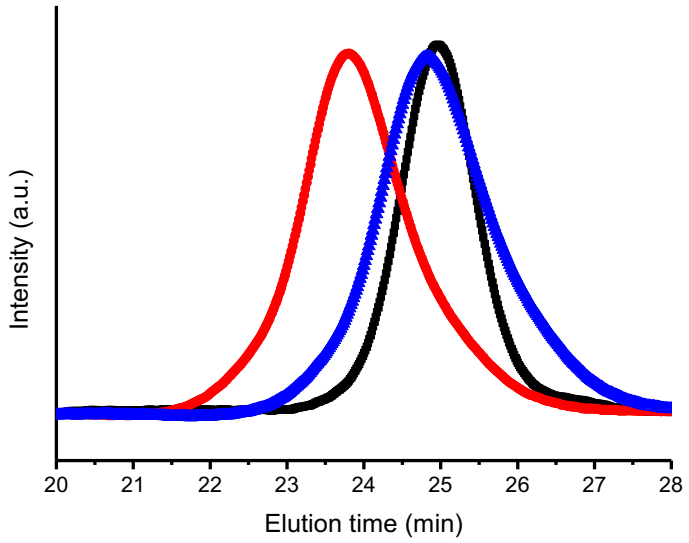

Figure S7. SEC traces of $[(BG)_5\text{-}(TBG)_5]_4$ (black), $[(BG)_5\text{-}(GalG)_5]_4$ (red) and $[(GA)_5\text{-}(GalG)_5]_4$ (blue).

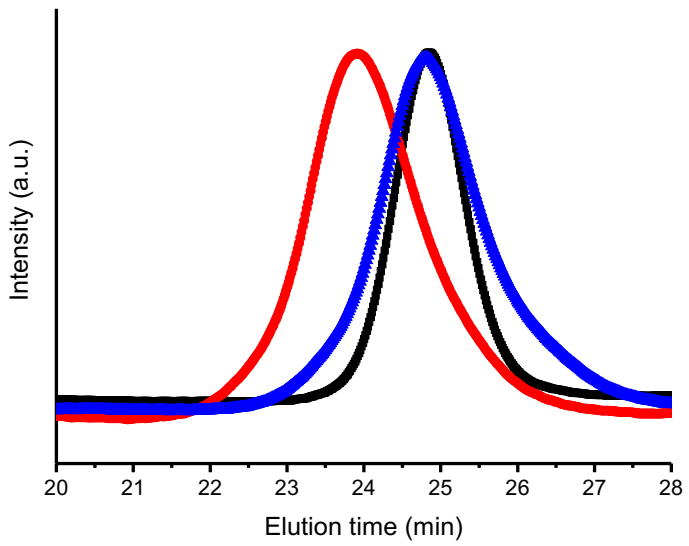

Figure S8. SEC traces of $(BG)_{20}$-*st*-$(TBG)_{20}$ (black), $(BG)_{20}$-*st*-$(GalG)_{20}$ (red) and $(GA)_{20}$-*st*-$(GalG)_{20}$ (blue).

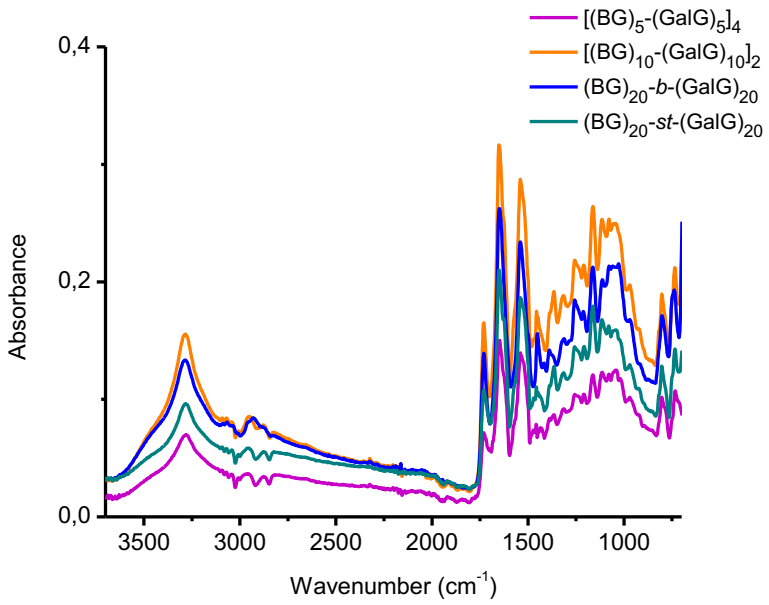

Figure S9. ATR-FTIR of solid glycopolypeptides with BG and GalG units.

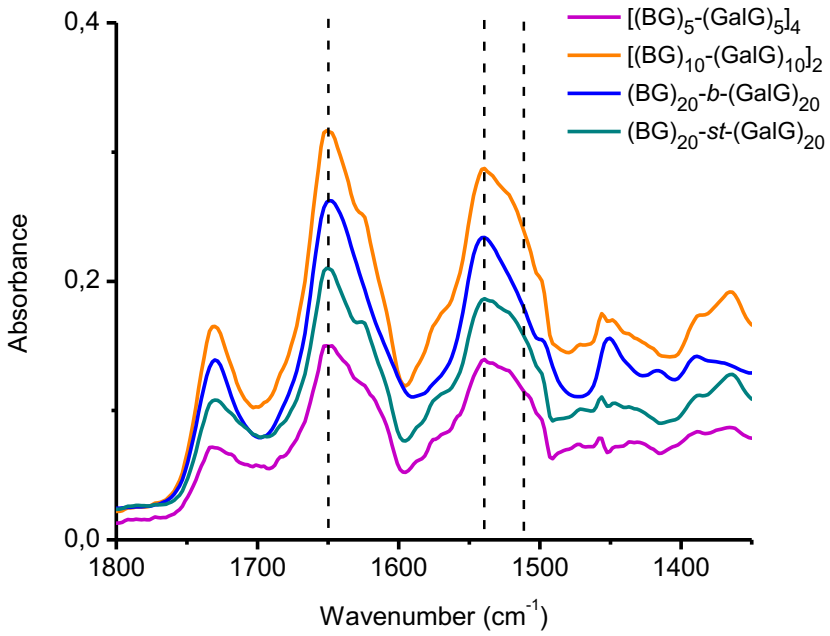

Figure S10. ATR-FTIR of solid glycopolypeptides with BG and GalG units, showing the 1800-1350 cm^{-1} region. The dashed lines indicate the expected position of Amide I and Amide II bands of α-helix structure.[i]

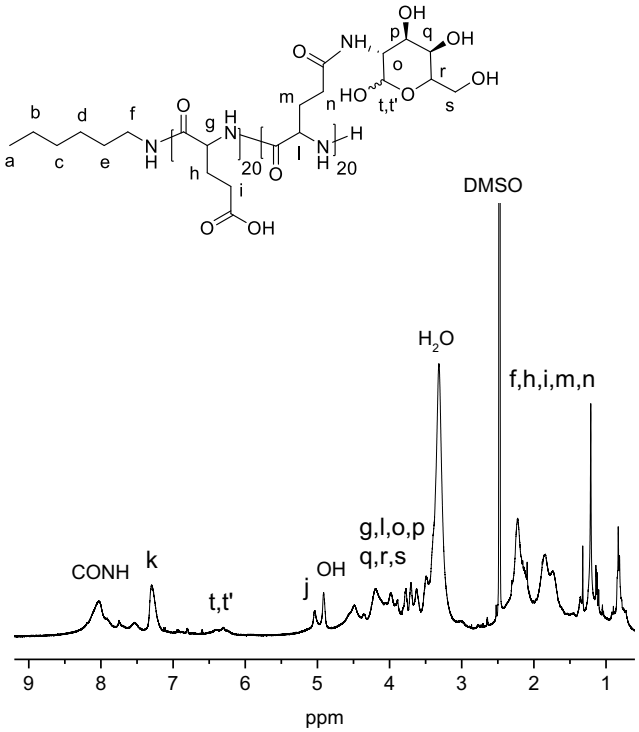

Figure S11. ^{1}H NMR of $(GA)_{20}$-*b*-$(GalG)_{20}$ in DMSO-*d*. The *j* and *k* signals correspond to residual benzyl ester groups (Figure S1).

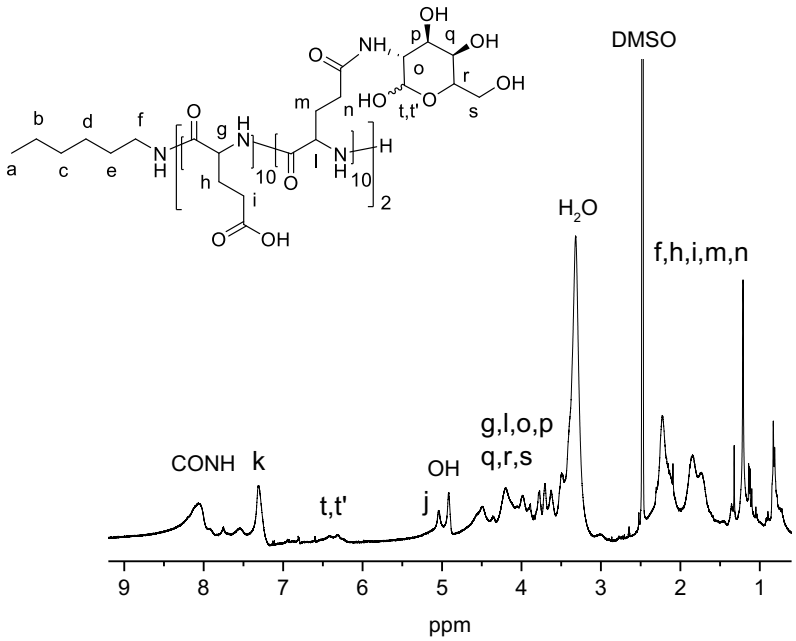

Figure S12. ^{1}H NMR of $[(GA)_{10}\text{-}(GalG)_{10}]_2$ in DMSO-*d*. The *j* and *k* signals correspond to residual benzyl ester groups (Figure S2).

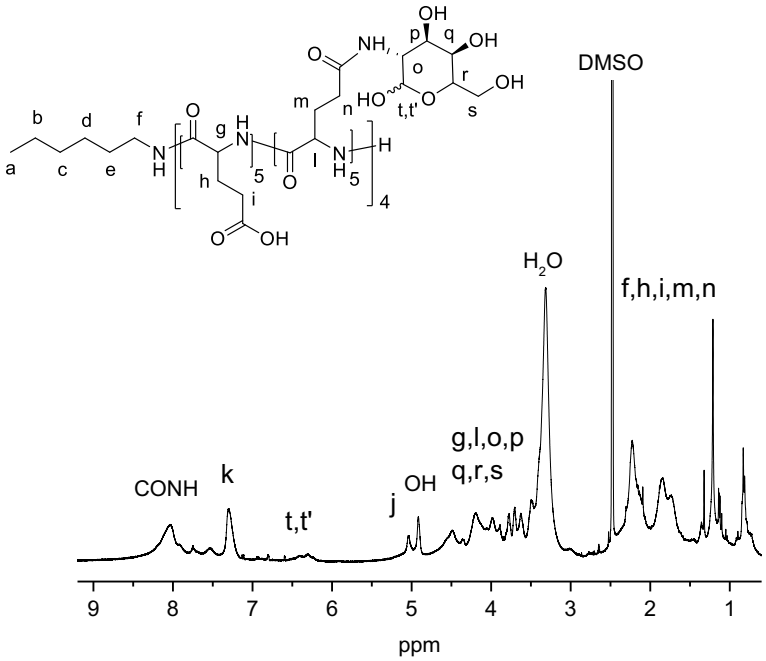

Figure S13. ^{1}H NMR of $[(GA)_5\text{-}(GalG)_5]_4$ in DMSO-*d*. The *j* and *k* signals correspond to residual benzyl ester groups (Figure S3).

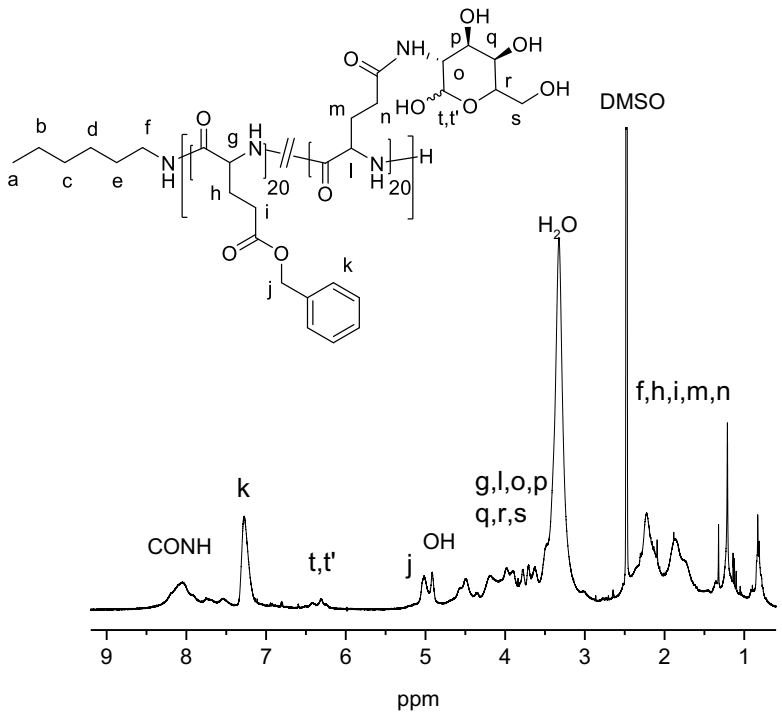

Figure S14. ^{1}H NMR of $(GA)_{20}$-*st*-$(GalG)_{20}$ in DMSO-*d*. The *j* and *k* signals correspond to residual benzyl ester groups (Figure S4).

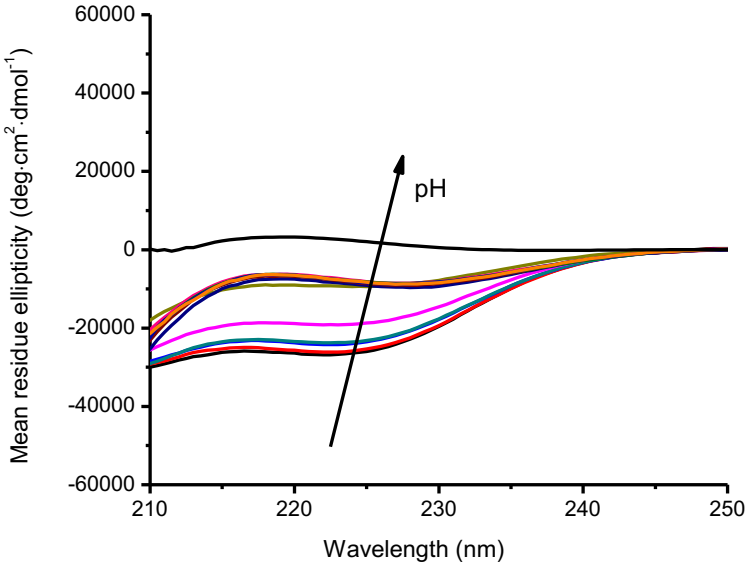

Figure S15. CD spectra of $[(GA)_5$-$(GalG)_5]_4$ upon increasing pH from 3 to 12.

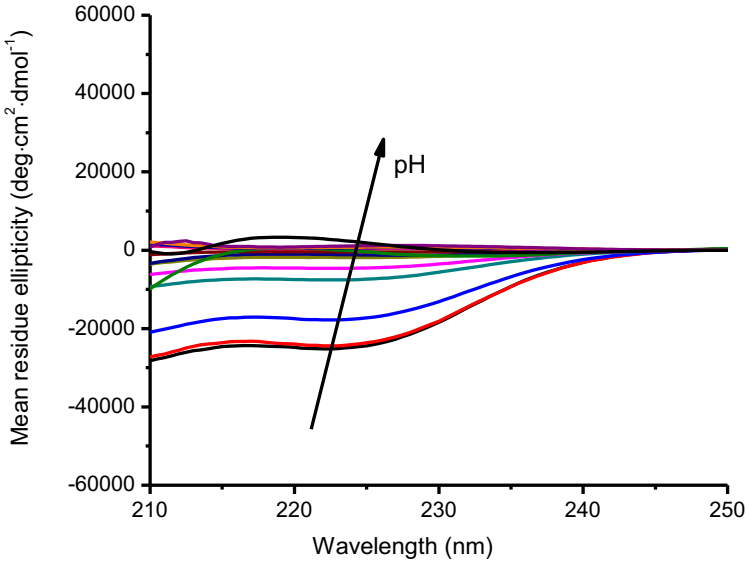

Figure S16. CD spectra of $[(GA)_{10}\text{-}(GalG)_{10}]_2$ upon increasing pH from 3 to 12.

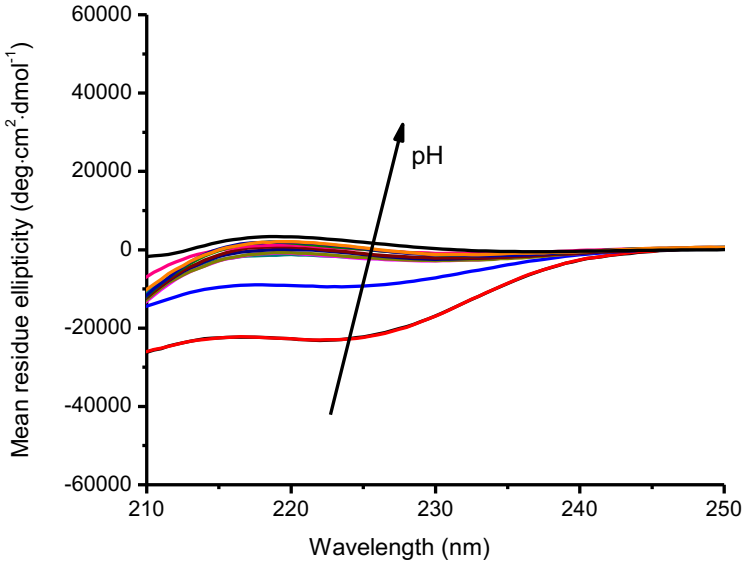

Figure S17. CD spectra of $(GA)_{20}$-*b*-$(GalG)_{20}$ upon increasing pH from 3 to 12.

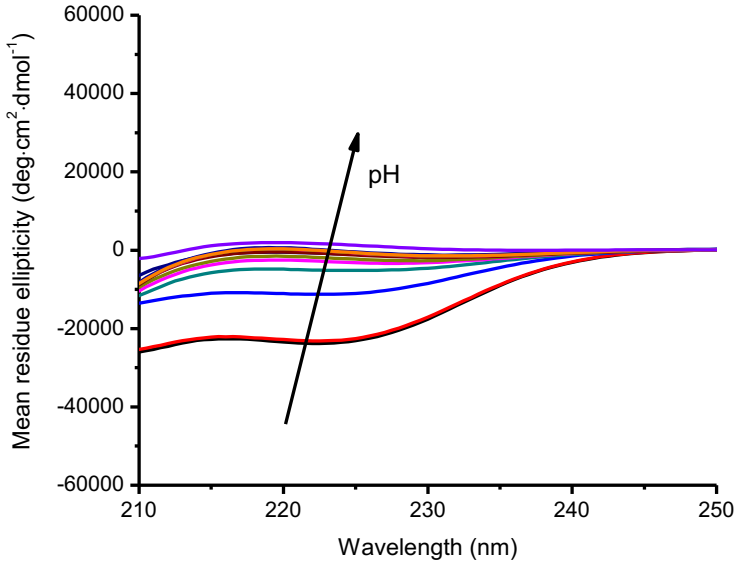

Figure S18. CD spectra of $(GA)_{20}$-*st*-$(GalG)_{20}$ upon increasing pH from 3 to 12.

References

[i] Miyazawa, T.; Blout, E.R. The infrared spectra of polypeptides with various conformations: amide I and amide II bands. *J. Am. Chem. Soc.* **1961**, *83*, 712-719.